J|A|C|S
ARTICLES
Published on Web 02/21/2002

Relativistic Spin−Orbit Coupling Effects on Secondary Isotope Shifts of ^{13}C Nuclear Shielding in CX_2 (X = O, S, Se, Te)

Perttu Lantto,[†] Juha Vaara,[*] Anu M. Kantola,[‡] Ville-Veikko Telkki,[‡] Bernd Schimmelpfennig,[§] Kenneth Ruud,[||] and Jukka Jokisaari[⊥]

Contribution from the NMR Research Group, Department of Physical Sciences, P.O. Box 3000, FIN-90014 University of Oulu, Finland, Department of Chemistry, P.O. Box 55, FIN-00014 University of Helsinki, Finland, Theoretical Chemistry, Teknikringen 30, Royal Institute of Technology, S-10044 Stockholm, Sweden, and Institute of Chemistry, Faculty of Science, University of Tromsø, N-9037 Tromsø, Norway

Received July 3, 2001. Revised Manuscript Received November 26, 2001

Abstract: Rovibrational corrections, temperature dependence, and secondary isotope shifts of the ^{13}C nuclear shielding in CX_2 (X = O, S, Se, Te) are calculated taking into account the relativistic spin−orbit (SO) interaction. The SO effect is considered for the first time for the secondary isotope shifts. The nuclear shielding hypersurface in terms of nuclear displacements is calculated by using a density-functional theory method. Ab initio multiconfiguration self-consistent field calculations are done at the equilibrium geometry for comparison. ^{13}C NMR measurements are carried out for CS_2. The calculated results are compared with both present and earlier experimental data on CO_2, CS_2, and CSe_2. The heavy-atom SO effects on the rovibrational corrections of ^{13}C shielding are shown to be significant. For CSe_2 and CTe_2, reliable prediction of secondary isotope effects and their temperature dependence requires the inclusion of the SO corrections. In particular, earlier discrepancies of theory and experiment for CSe_2 are fully resolved by taking the SO interactions into account.

1. Introduction

The molecular electronic properties accessible to NMR spectroscopy are thermal averages over the rovibrational motion of the nuclei. Parameters such as nuclear shieldings (corresponding to observable chemical shifts) contain information about the zero-point vibrations, the effect of temperature, and the different nuclear isotopes.[1−4] Isotope effects may be classified into two categories. The primary isotope effect on the nuclear shielding is the change due to isotopic substitution of the observed nucleus itself. The secondary isotope effects arise when the isotope of another nucleus in the molecule is changed. In general, the mass increase of the X nucleus results in shorter average XA bond length. For main-group nonmetallic elements, this typically leads to higher average shielding $\langle\sigma_A\rangle$ of the nucleus A.[5,6] This implies positive one-bond isotope shifts, $\langle\sigma_A(^{M'}X)\rangle - \langle\sigma_A(^{M}X)\rangle$, with $M' > M$, where M and M' are the mass numbers of the different isotopes of the neighboring nucleus X.

NMR parameters are quite sensitive to relativistic effects in systems containing heavy atoms. This is due to the contributions arising from the heavy-atom core regions where the velocity of the electrons is high.[7] The dominating relativistic effect on the shielding of light nuclei, the spin−orbit (SO) coupling,[8−10] can be theoretically calculated with several electronic structure methods. They include unrestricted Hartree−Fock (UHF),[11] density-functional theory (DFT),[12−14] and multiconfigurational self-consistent field (MCSCF)[15,16] approaches, as well as fully

* Corresponding author. Department of Chemistry, P.O. Box 55 (A. I.Virtasen aukio 1), FIN-00014 University of Helsinki, Finland. E-mail: jvaara@chem.helsinki.fi.
[†] University of Oulu. E-mail: Perttu.Lantto@oulu.fi.
[‡] University of Oulu.
[§] Royal Institute of Technology.
[||] University of Tromsø.
[⊥] University of Oulu. E-mail: Jukka.Jokisaari@oulu.fi.

(1) Jameson, C. J. In *Theoretical models of Chemical Bonding, Part 3. Molecular Spectroscopy, Electronic Structure, and Intermolecular Interactions*; Maksic, Z. B., Ed.; Springer: Berlin, 1991; p 457.
(2) Hansen, P. *Prog. NMR Spectrosc.* **1988**, *20*, 207.
(3) *NMR Basic Principles and Progress 22: Isotope effects in NMR Spectroscopy*; Diehl, P., Fluck, E., Günther, G., Kosfeld, R., Seelig, J., Eds.; Springer: Berlin, 1990.
(4) Jameson, C. J. In *Isotopes in the Physical and Biomedical Sciences*; Buncel, E., Jones, K., Eds.; Elsvier: Amsterdam, 1990.
(5) Webb, G. A. In *Nuclear Magnetic Shielding and Molecular Structure*; Tossel, J. A., Ed.; Kluwer: Dordrecht, 1993.
(6) Jameson C. J.; Dios, A. C. In *Nuclear Magnetic Shielding and Molecular Structure*; Tossel J. A., Ed.; Kluwer: Dordrecht, 1993.
(7) Pyykkö, P. *Adv. Quantum Chem.* **1978,** *11*, 353; *Chem. Rev.* **1988**, *88*, 563.
(8) Nomura, Y.; Takeuchi, Y.; Nakagawa, N. *Tetrahedron Lett.* **1969**, *8*, 639.
(9) Pyykkö, P.; Görling, A.; Rösch, N. *Mol. Phys.* **1987**, *61*, 195.
(10) Kaupp, M.; Malkina, O. L.; Malkin, V. G.; Pyykkö, P. *Chem.-Eur. J.* **1998**, *4*, 118.
(11) Nakatsuji, H.; Takashima, H.; Hada, M. *Chem. Phys. Lett.* **1995**, *233*, 95.
(12) Malkin, V. G.; Malkina, O. L.; Salahub, D. R. *Chem. Phys. Lett.* **1996**, *261*, 335.
(13) Wolff S. K.; Ziegler, T. *J. Chem. Phys.* **1998**, *109*, 895.
(14) Malkina, O. L.; Schimmelpfennig, B.; Kaupp, M.; Hess, B. A.; Chandra, P.; Wahlgren, U.; Malkin, V. G. *Chem. Phys. Lett.* **1998**, *296*, 93.
(15) Vaara, J.; Ruud, K.; Vahtras, O.; Ågren, H.; Jokisaari, J. *J. Chem. Phys.* **1998**, *109*, 1212.
(16) Vaara, J.; Ruud, K.; Vahtras, O. *J. Chem. Phys.* **1999**, *111*, 2900.

10.1021/ja016537+ CCC: $22.00

relativistic four-component methods.[17,18] In third-order perturbation theory based on a nonrelativistic (NR) reference state, the SO interaction couples the singlet ground state with triplet excited states through the Fermi contact (FC) and spin−dipole (SD) hyperfine interactions. Simultaneously, the second-order SO effect arising from the interaction the FC and SD operators with the magnetic field dependent part of the SO operator should be taken into account.[16,19]

The SO effect on nuclear shielding is strongly dependent on the chemical surroundings of the nucleus and the molecular geometry, as demonstrated by Minaev et al.[20] for the hydrogen halide (HX, X = Cl, Br, I) series of molecules. It was found that the SO effect on the ^{1}H shielding increases with increasing bond length, becoming numerically larger than the NR shielding at long distances for HI. This stems from the shared dissociation limit for the singlet ground state and a triplet excited state, implying decreasing triplet excitation energy with increasing bond length. It is mainly the strong geometry dependence of the so-called FC(1) term,[20] arising from the triplet Fermi contact/one-electron SO interaction, which causes this effect.

As shown in ref 20, the SO interaction produces qualitative changes in the effects of rovibrational motion on the shieldings. However, the changes are difficult to measure through the temperature dependence of the absolute shielding or primary isotope effects. The former necessitates a good absolute shielding scale for the nucleus in question, i.e., a reference molecule where the absolute shielding is known for all temperatures investigated. Also the effects of the solvent on both the reference molecule and the molecule under investigation have to be known in order to obtain reliable experimental values. In the case of primary isotope effects, the problem lies in the different frequency scales of the measurements for the two nuclear isotopes. In contrast, secondary isotope effects are more easily accessible experimentally as they cause fine structure in the NMR spectrum of the observed nucleus.

The subject of this work is the influence of the SO interaction on the secondary isotope effects of ^{13}C nuclear shieldings in the CX_2 (X = O, S, Se, Te) molecules, due to isotopic substitution of X. The effect of temperature on absolute shieldings will also be considered. CX_2 is an interesting series of molecules, as previous work[21] was unable to reach quantitative agreement between experimental and nonrelativistically determined theoretical ^{13}C isotope shifts for CSe_2. Large SO effects are expected in molecules containing heavy chalcogens such as selenium and tellurium. The calculations involve averaging the nuclear shielding hypersurface through nuclear motion governed by the potential energy hypersurface.[1] Most of the present calculations are carried out using the DFT approach,[12,14,22,23] as it is both computationally expedient and expected to produce a shielding hypersurface accurate enough for estimating the isotope effects. For comparison, we use MCSCF[15,16,24] calculations at the equilibrium geometry. Experimental secondary one-bond isotope effects on ^{13}C shielding in CS_2 are also determined.

2. Theory

2.1. Nuclear Magnetic Shielding. The magnetic field seen by the magnetic moment of nucleus K in a molecule is different from the external field applied by the NMR spectrometer. The modification, due to the electron cloud, is characterized by the nuclear shielding tensor $\boldsymbol{\sigma}_K$, whose Cartesian $\epsilon\tau$-component has four contributions when the relativistic SO effects are taken into account perturbationally,[15,16]

$$\sigma_{\epsilon\tau} = \sigma^d_{\epsilon\tau} + \sigma^p_{\epsilon\tau} + \sigma^{\mathrm{SO-I}}_{\epsilon\tau} + \sigma^{\mathrm{SO-II}}_{\epsilon\tau} \quad (1)$$

The first term is computable as a ground-state expectation value. Together with the second-order paramagnetic term $\sigma^p_{\epsilon\tau}$—which can be calculated as a linear response of the wave function with respect to the magnetic field perturbation—they constitute the NR shielding, $\sigma^{\mathrm{NR}}_{\epsilon\tau} = \sigma^d_{\epsilon\tau} + \sigma^p_{\epsilon\tau}$.[25] The sum is formally gauge-invariant and the contributing quantum mechanical operators do not involve the electron spin.

The third-order SO correction

$$\sigma^{\mathrm{SO-I}}_{\epsilon\tau} = \sigma^{\mathrm{FC(1)}}_{\epsilon\tau} + \sigma^{\mathrm{FC(2)}}_{\epsilon\tau} + \sigma^{\mathrm{SD(1)}}_{\epsilon\tau} + \sigma^{\mathrm{SD(2)}}_{\epsilon\tau} \quad (2)$$

arises from the one- and two-electron components of the field-free electronic SO Hamiltonian [the terms with (1) and (2), respectively].[8−10] H_{SO} creates spin polarization, through admixture of triplet excited states, into the singlet ground state. This spin polarization is then detected by the nucleus−electron hyperfine interactions involving the electronic spin variable, i.e., the triplet FC or SD operators. The coupling to the applied magnetic field occurs through the orbital Zeeman interaction. The third-order Rayleigh−Schrödinger perturbation theory (PT) expressions involved in the terms of eq 2 can be evaluated either analytically as quadratic response functions[26] or by lowering the analytical PT order by using finite perturbation theory (FPT) for one of the interactions.[11,12]

In the second-order SO contribution[16,19]

$$\sigma^{\mathrm{SO-II}}_{\epsilon\tau} = \sigma^{\mathrm{FC-II(1)}}_{\epsilon\tau} + \sigma^{\mathrm{FC-II(2)}}_{\epsilon\tau} + \sigma^{\mathrm{SD-II(1)}}_{\epsilon\tau} + \sigma^{\mathrm{SD-II(2)}}_{\epsilon\tau} \quad (3)$$

the coupling to the magnetic field is provided by the magnetic field dependence of the SO operator itself. These are obtained by applying the minimal substitution[27] of the contribution of the magnetic vector potential (corresponding to the external field) to the momentum and, hence, angular momentum operators appearing in the SO interaction. The resulting terms are analogous to the gauge correction terms of the g-tensor of electron paramagnetic resonance spectroscopy.[28] They can be calculated either analytically as triplet linear response functions[26] or again by FPT.[22] The sum of the corresponding SO-I and SO-II terms is formally gauge-invariant in analogy with the NR

(17) Ishikawa, Y.; Nakajima, T.; Hada, M.; Nakatsuji, H. *Chem. Phys. Lett.* **1998**, *283*, 119.
(18) Visscher, L.; Enevoldsen, T.; Saue, T.; Jensen, H. J. Aa.; Oddershede, J. *J. Comput. Chem.* **1999**, *20*, 1262.
(19) Fukui, H.; Baba, T.; Inomata, H. *J. Chem. Phys.* **1996**, *105*, 3175; **1997**, *106*, 2987.
(20) Minaev, B.; Vaara, J.; Ruud, K.; Vahtras, O.; Ågren, H. *Chem. Phys. Lett.* **1998**, *295*, 455. See also: Cromp, B.; Carrington, T., Jr.; Salahub, D. R.; Malkina, O. L.; Malkin, V. G. *J. Chem. Phys.* **1999**, *110*, 7153.
(21) Lounila, L.; Vaara, J.; Hiltunen, Y.; Pulkkinen, A.; Jokisaari, J.; Ala-Korpela, M.; Ruud, K. *J. Chem. Phys.* **1997**, *107*, 1350.
(22) Vaara, J.; Malkina, O. L.; Stoll, H.; Malkin, V. G.; Kaupp, M. *J. Chem. Phys.* **2001**, *114*, 61.
(23) Malkin, V. G.; Malkina, O. L.; Casida, M. E.; Salahub, D. R. *J. Am. Chem. Soc.* **1994**, *116*, 5898.
(24) Ruud, K.; Helgaker, T.; Kobayashi, R.; Jørgensen, P.; Bak, K. L.; Jensen, H. J. Aa. *J. Chem. Phys.* **1994**, *100*, 8178.
(25) Ramsey, N. F. *Phys. Rev.* **1950**, *78*, 699; **1952**, *86*, 243.
(26) Olsen, J.; Jørgensen, P. *J. Chem. Phys.* **1985**, *82*, 3235.
(27) Atkins, P. W.; Friedman, R. S. *Molecular Quantum Mechanics*, 3rd ed.; Oxford University Press: New York, 1997.
(28) Harriman, J. E. *Theoretical Foundations of Electron Spin Resonance*; Academic: New York, 1978.

shielding.[19] Hence, FC-II(n) and SD-II(n) may be called diamagnetic contributions to the SO correction to nuclear shieldings. We refer to the original papers[15,16] and references therein for further details.

2.2. Isotope and Temperature Effects. To compare theoretically calculated shieldings to experimental values, one needs to perform rovibrational averaging. One way of doing this is to expand the parameter as a Taylor series in terms of the internal displacement coordinates ΔR_i (of bond lengths and angles etc.) around the equilibrium geometry.[1] There are four relevant coordinates in a linear XAX′-type molecule: AX and AX′ bond stretching coordinates, Δr and $\Delta r'$, as well as two bending coordinates, $\Delta\theta$ and $\Delta\theta'$, in the xz and yz planes, when the molecule is along the z axis. Neglecting third- and higher-order terms (as their contribution to the total rovibrational effect is small[1]), the expression for the thermally averaged shielding constant of nucleus A at temperature T is

$$\langle\sigma\rangle^T = \sigma_e + \sigma_r[\langle\Delta r\rangle^T + \langle\Delta r'\rangle^T] + \frac{1}{2}\sigma_{rr}[\langle(\Delta r)^2\rangle^T + \langle(\Delta r')^2\rangle^T] + \sigma_{rr'}\langle\Delta r\Delta r'\rangle^T + \frac{1}{2}\sigma_{\theta\theta}[\langle(\Delta\theta)^2\rangle^T + \langle(\Delta\theta')^2\rangle^T] \quad (4)$$

where σ_e is the shielding constant at the equilibrium geometry and σ_{R_i} and $\sigma_{R_iR_j}$ are the first and second derivatives, respectively, of the shielding constant with respect to the displacement coordinates, taken at the equilibrium geometry. These parameters define the shielding hypersurface. All other first- and second-order terms vanish due to the symmetry of the linear CX_2 systems. These and other derivatives of scalar properties are independent of nuclear masses and temperature in the Born−Oppenheimer approximation. As the rovibrational motion of a molecule depends on these quantities, so do also the thermal average values of the displacement coordinates, $\langle\Delta R_i\rangle^T$ and $\langle\Delta R_i\Delta R_j\rangle^T$. To calculate these to leading order, both the harmonic (quadratic) ($f_{R_iR_j}$) and cubic anharmonic ($f_{R_iR_jR_k}$) force constants are needed. Up to this level, the energy function for a linear XAX′ molecule can be written down as

$$V = \frac{1}{2}f_{rr}[(\Delta r)^2 + (\Delta r')^2] + f_{rr'}\Delta r\Delta r' + \frac{1}{2}f_{\theta\theta}[(\Delta\theta)^2 + (\Delta\theta')^2] + \frac{1}{6}f_{rrr}[(\Delta r)^3 + (\Delta r')^3] + \frac{1}{2}f_{rrr'}\Delta r\Delta r'(\Delta r + \Delta r') + \frac{1}{2}f_{r\theta\theta}(\Delta r + \Delta r')[(\Delta\theta)^2 + (\Delta\theta')^2] \quad (5)$$

The curvilinear ΔR_i coordinates are related to the rectilinear vibrational normal coordinates Q_k by a nonlinear transformation involving the so-called L-tensors.[29] The rovibrational averages $\langle Q_k\rangle^T$ and $\langle Q_k^2\rangle^T$ can be calculated using well-known formulas.[30,31] The latter are obtained from the zero-order wave function of the harmonic oscillator, i.e., averaged over the harmonic vibrations of the molecule. $\langle Q_k\rangle^T$ are influenced by both vibration and rotation of the molecule. Whereas the part resulting from the vibrational anharmonicity is calculated from the first-order wave functions perturbed by the cubic force field, a classical equipartition of the energy argument is used for the rotational (centrifugal distortion) part.[30]

(29) Hoy, A. R.; Mills, I. M.; Strey, G. *Mol. Phys.* **1972**, *24*, 1265.
(30) Toyama, M.; Oka, T.; Morino, Y. *J. Mol. Spectrosc.* **1964**, *13*, 193.
(31) Lounila, J.; Wasser, R.; Diehl, P. *Mol. Phys.* **1987**, *62*, 19.

3. Computational Details

3.1. DFT Calculations. DFT calculations of shielding hypersurfaces have been carried out using a local version of the deMon program[32] which includes the corresponding NMR modules.[22,23,33] NR shieldings were calculated by using the individual gauge for the localized orbitals (IGLO) method[34] with the Perdew/Wang PW91 exchange-correlation functional.[35] The integration grid of deMon was with the EXTRAFINE angular quadrature and 128 radial points per atom (E128).[32]

The SO corrections were calculated with the Breit−Pauli one-electron/one-center mean-field approximation[14,36] for the one- and two-electron SO operators using the AMFI code.[37] The FC operator on the carbon nucleus was included in the zero-order self-consistent Hamiltonian as a finite perturbation.[12,22] The corresponding FPT parameter, $\lambda_C = 0.003$, was chosen on the basis of the observed plateau of stable results. The terms involving the SD operator were neglected in the present DFT calculations for both computational convenience and the fact that the SO effects usually are dominated by the FC interaction.[11,15,16] Similarly, the diamagnetic FC-II(2) gauge correction term was not calculated due to the lack of an efficient way to calculate the corresponding molecular integrals. Its effect is most likely small, judged by the results for the electronic g-tensor.[38]

We used both the common gauge origin (CGO) at the carbon nucleus and the IGLO gauge. An earlier exchange functional by Perdew and Wang as well as the correlation functional by Perdew (P86)[39] were used, as they have been shown to provide reasonable accuracy in calculations involving the FC interaction.[33,40,41] The IGLO localization was performed, as in the NR case, using the Pipek−Mezey (PM) algorithm[42] (IGLO PM[43]). The E128 grid was used. CGO was only employed at the equilibrium geometry in order to produce results comparable with the MCSCF calculations (see below). The dependence of the results on the location of the CGO was investigated by placing the gauge origin to the X nucleus instead of carbon and found to be negligible with the present basis sets.

The Loc.1 approximation of the sum-over-states density-functional perturbation theory (SOS-DFPT) approach[23] was employed in all calculations. We refer to the original paper for details.

We used the basis sets of Huzinaga,[44] contracted and polarized by Kutzelnigg et al.,[34] and denoted HIII for C, O, and S. The Se and Te basis sets are due to Fægri[45] and were used with the same type of contraction pattern and polarization functions as in the HIII basis sets for the lighter elements. In the [primitive/contracted] notation the basis

(32) Salahub, D. R.; Fournier, R.; Mlynarski, P. Papai, I. St-Amant, A.; Ushio, J. In *Density Functional Methods in Chemistry*; Labanowski, J., Andzelm, J., Eds.; Springer: New York, 1991. St-Amant, A.; Salahub, D. R. *Chem. Phys. Lett.* **1990**, *169*, 387. St-Amant, A. Thesis, Université de Montréal, 1992.
(33) Malkin, V. G.; Malkina, O. L.; Eriksson, L. A.; Salahub, D. R. In *Modern Density Functional Theory: A Tool for Chemistry*, Vol. 2 of *Theoretical and Computational Chemistry*; Politzer, P., Seminario, J. M., Eds.; Elsevier: Amsterdam, 1995; p 273.
(34) Kutzelnigg, W.; Fleischer, U.; Schindler, M. In *NMR Basic Principles and Progress 23*; Diehl, P., Fluck, E., Günther, H., Kosfeld, R., Seelig, J., Eds.; Springer: Berlin, 1990.
(35) Perdew, J. P.; Wang, Y. *Phys. Rev. B* **1992**, *45*, 13244. Perdew, J. P.; Chevary, J. A.; Vosko, S. H.; Jackson, K. A.; Pederson, M. R.; Singh, D. J.; Fiolhais, C. *Phys. Rev. B* **1992**, *46*, 6671.
(36) Hess, B. A.; Marian, C. M.; Wahlgren, U.; Gropen, O. *Chem. Phys. Lett.* **1996**, *251*, 365.
(37) Schimmelpfennig, B. *Atomic spin−orbit Mean-Field Integral program*, Stockholms Universitet, 1996.
(38) Lushington, G. H.; Grein, F. *Theor. Chem. Acc.* **1996**, *93*, 259.
(39) Perdew, J. P.; Wang, Y. *Phys. Rev. B* **1986**, *33*, 8800. Perdew, J. P. *Phys. Rev. B* **1986**, *33*, 8822.
(40) Malkin, V. G.; Malkina, O. L.; Salahub, D. R. *Chem. Phys. Lett.* **1994**, *221*, 91. Malkina, O. L.; Salahub, D. R.; Malkin, V. G. *J. Chem. Phys.* **1996**, *105*, 8793.
(41) Eriksson, L. A.; Malkina, O. L.; Malkin, V. G.; Salahub, D. R. *J. Chem. Phys.* **1994**, *100*, 5066.
(42) Pipek, J.; Mezey, P. G. *J. Chem. Phys.* **1989**, *90*, 4916.
(43) Kaupp, M.; Malkina, O. L.; Malkin, V. G. *J. Chem. Phys.* **1997**, *106*, 9201.
(44) Huzinaga, S. *Approximate Atomic Functions*, University of Alberta, Edmonton, 1971.
(45) Fægri, K., personal communication.

sets are [11s7p2d/7s6p2d] for C and O, [12s8p3d/8s7p3d] for S, [16s13p11d/12s11p11d] for Se, and [20s16p14d/14s13p12d] for Te. Spherical Gaussian functions are used throughout.

For the fitting of the charge density and exchange-correlation potentials using Gaussian functions, we used auxiliary basis sets denoted as (5,2;5,2) for C and O, (5,4;5,4) for S, and (5,5;5,5) for Se and Te. The first two numbers in the notation are the number of s-primitives and spd-shells (sharing a common exponent), respectively, for the charge density. The last two numbers denote the same for the exchange-correlation potential.

3.2 MCSCF Calculations. Restricted active space (RAS)[46] calculations were carried out at the equilibrium geometry using the DALTON quantum chemistry program.[47] The active molecular orbital (MO) spaces were ${}^{2000\ 1000}_{2000\ 2000}\mathrm{RAS}^{0220\ 0110}_{2000\ 2110}$ for CO_2, ${}^{4110\ 3110}_{2000\ 2000}\mathrm{RAS}^{0220\ 0110}_{3001\ 2111}$ for CS_2, ${}^{8331\ 7331}_{2000\ 2000}\mathrm{RAS}^{0220\ 0110}_{3001\ 2111}$ for CSe_2, and ${}^{12,552\ 11,552}_{2000\ 2000}\mathrm{RAS}^{0220\ 0110}_{3001\ 2111}$ for CTe_2, in the ${}^{\mathrm{inactive}}_{\mathrm{RAS1}}\mathrm{RAS}^{\mathrm{RAS2}}_{\mathrm{RAS3}}$ notation. The numbers denote molecular orbitals in each of the A_g, B_{3u}, B_{2u}, B_{1g}, B_{1u}, B_{2g}, B_{3g}, and A_u irreducible representations of the D_{2h} point group, respectively. These balanced active spaces were chosen by inspection of the MP2 natural orbital occupation numbers.[48] The two highest doubly degenerate occupied orbitals as well as the doubly degenerate lowest unoccupied orbital were in the RAS2 orbital subspace. A full configuration interaction is performed in this restricted space. This is essential in order to be able to describe static electron correlation effects. The other occupied and virtual MO's mostly affected by correlation (as judged from the MP2 occupations) were placed in the RAS1 and RAS3 subspaces, respectively. Single and double excitations were allowed out of RAS1 and into RAS3, in an attempt to capture some of the dynamical correlation effects. The inactive MO's are subject to optimization but are not correlated.

Two calculations were performed for CO_2 and CS_2, one with the HIII basis sets for all nuclei as well as a locally dense one where the HIVu3 set was used for C and HIV for O and S. This mixed basis is denoted here as HIVu3/HIV. The HIV basis[34,44] is [11s7p3d1f/8s7p3d1f] for C and O and [12s8p4d2f/9s8p4d2f] for S. The HIVu3 set is obtained from HIV by full decontraction and supplementing this basis with three tight (high-exponent) s-type primitive Gaussians. The exponents were obtained by multiplication of the highest existing exponent by the factor of 3. The purpose of adding tight basis functions is to improve the description of the FC perturbation. In CSe_2 and CTe_2, the HII basis[45] was used for Se and Te. These sets are [16s13p10d/11s10p10d] for Se and [20s16p13d/13s12p10d] for Te. They were used in a locally dense manner with both HIII and HIVu3 basis sets for carbon. This procedure is dictated by software limitations in correlated calculations of nuclear shieldings.

The NR shieldings were calculated by using gauge-including atomic orbitals (GIAO's).[24] For the third-order SO contributions, we adopted the fully analytical approach[15] that uses the triplet quadratic response function.[26,49] Triplet linear response functions[50] are needed in the analytical method[16] used to compute the second-order SO corrections. All SO contributions are obtained with a CGO placed at carbon, and the results are expected to be practically independent of the location of the CGO. As in the DFT calculations, the FC-II(2) and SD-II(2) terms involving the two-electron gauge correction integrals were neglected. All the other terms involving both FC and SD hyperfine operators were retained, however, in contrast to the DFT work. The mean-field SO integrals from the AMFI code were used.

3.3. Isotope and Temperature Effects. The equilibrium molecular structures were optimized with the GAUSSIAN98 program[51] at the MP2 level, using quasi-relativistic large-core effective core potentials (RECP).[52] Uncontracted valence basis sets[53] supplemented with two d-exponents from the HIII set, were used. The sets were (4s4p2d) for C and O and (4s5p2d) for S, Se, and Te. The harmonic and cubic force constants were obtained by fitting eq 5—including also the all-diagonal fourth-order constants—to the total energy values at the equilibrium geometry and 14 geometries slightly displaced from the equilibrium. The theoretical level was the same as for the geometry optimizations. The RECPs are expected to give a reliable force field for molecules containing heavy atoms (Se and Te) as scalar relativistic effects are taken into account by this technique. RECPs were used for all systems in the present series to obtain a consistent quality of the force fields.

The calculations of the thermal average displacement coordinates $\langle \Delta R_i \rangle^T$ and $\langle \Delta R_i \Delta R_j \rangle^T$ were performed by using the AVIBR program.[31] The derivatives of the ^{13}C nuclear shielding constants with respect to the displacement coordinates were obtained by fitting the property surface of eq 4—supplemented with the full third-order surface—to the shieldings from DFT calculations at 12 different geometries (including the equilibrium), suitably chosen near the MP2/RECP equilibrium geometry.

3.4. Experimental Section. NMR measurements were done on natural abundance CS_2. The sample was prepared into a standard 5-mm o.d. NMR tube with ca. 20 vol % of $CDCl_3$ as a lock substance and 1atm of $^{13}CH_4$ as an internal chemical shift reference. The ^{13}C spectra were recorded at several temperatures with the Bruker Avance DRX 500 spectrometer (corresponding to the resonance frequency of 125.76 MHz for ^{13}C). Temperature was calibrated with a standard calibration sample of ethylene glycol that gives an accuracy of $\pm 1°$. To obtain signals from both the molecule under study and the reference molecule, a spectral window of 30 kHz was used, digital resolution being 0.06 Hz. To observe the extremely small temperature dependence of the isotope shift, additional spectra around the $^{13}CS_2$ region were measured using a 0.5 kHz spectral window with a digital resolution of 0.01 Hz. A total of 4096 scans were accumulated. This is enough to reveal signals arising from the four most abundant isotopomers. However, one of the four is almost masked by the strongest signal, making accurate analysis impossible for this particular signal. The number of scans collected for the temperature series was 128, with spectra showing only the two most prominent peaks. The line widths varied from 0.1 to 0.2 Hz.

Each spectrum was analyzed by using the total line-shape fitting mode of the PERCH software,[54] to obtain chemical shifts with standard deviations of 0.006 Hz (0.05 ppb) and 0.003 Hz (0.02 ppb) or better for the absolute shieldings and the isotope shifts, respectively. Both the chemical shifts (with respect to $^{13}CH_4$) and the isotope shifts were found to decrease linearly with temperature in the present temperature range.

(46) Olsen, J.; Roos, B. O.; Jørgensen, P.; Jensen, H. J. Aa. *J. Chem. Phys.* **1988**, *89*, 2185. Malmqvist, P.-Å.; Rendell, A.; Roos, B. O. *J. Phys. Chem.* **1990**, *94*, 5477.

(47) Helgaker, T.; Jensen, H. J. Aa.; Jørgensen, P.; Olsen, J.; Ruud, K.; Ågren, H.; Bak, K. L.; Bakken, V.; Christiansen, O.; Coriani, S.; Dahle, P.; Dalskov, E. K.; Enevoldsen, T.; Fernandez, B.; Hættig, C.; Hald, K.; Halkier, A.; Heiberg, H.; Hettema, H.; Jonsson, D.; Kirpekar, S.; Kobayashi, R.; Koch, H.; Mikkelsen, K. V.; Norman, P.; Packer, M. J.; Ruden, T. A.; Saue, T.; Sauer, S. P. A.; Schimmelpfennig, B.; Sylvester-Hvid, K. O.; Taylor, P. R.; Vahtras, O. Dalton release 1.2 2001, an electronic structure program. See http://www.kjemi.uio.no/software/dalton/dalton.html.

(48) Jensen, H. J. Aa.; Jørgensen, P.; Ågren, H.; Olsen, J. *J. Chem. Phys.* **1988**, *88*, 3834.

(49) Vahtras, O.; Ågren, H.; Jørgensen, P.; Jensen, H. J. Aa.; Helgaker, T.; Olsen, J. *J. Chem. Phys.* **1992**, *97*, 9178.

(50) Olsen, J.; Yeager, D. L.; Jørgensen, P. *J. Chem. Phys.* **1989**, *91*, 381.

(51) Frisch, M. J.; Trucks, G. W.; Schlegel, H. B.; Scuseria, G. E.; Robb, M. A.; Cheeseman, J. R.; Zakrzewski, V. G.; Montgomery, J. A., Jr.; Stratmann, R. E.; Burant, J. C.; Dapprich, S.; Millam, J. M.; Daniels, A. D.; Kudin, K. N.; Strain, M. C.; Farkas, O.; Tomasi, J.; Barone, V.; Cossi, M.; Cammi, R.; Mennucci, B.; Pomelli, C.; Adamo, C.; Clifford, S.; Ochterski, J.; Petersson, G. A.; Ayala, P. Y.; Cui, Q.; Morokuma, K.; Malick, D. K.; Rabuck, A. D.; Raghavachari, K.; Foresman, J. B.; Cioslowski, J.; Ortiz, J. V.; Stefanov, B. B.; Liu, G.; Liashenko, A.; Piskorz, P.; Komaromi, I.; Gomperts, R.; Martin, R. L.; Fox, D. J.; Keith, T.; Al-Laham, M. A.; Peng, C. Y.; Nanayakkara, N.; Gonzalez, C.; Challacombe, M.; Gill, P. M. W.; Johnson, B.; Chen, W.; Wong, M. W.; Andres, J. L.; Gonzalez, C.; Head-Gordon, M.; Replogle, E. S.; Pople, J. A. Gaussian 98, Revision A.3, Gaussian, Inc., Pittsburgh, PA, 1998.

(52) Bergner, A.; Dolg, M.; Küchle, W.; Stoll, H.; Preuss, H. *Mol. Phys.* **1993**, *80*, 1431.

(53) Kaupp, M.; Schleyer, P. v. R.; Stoll, H.; Preuss, H. *J. Am. Chem. Soc.* **1991**, *113*, 6012.

(54) Laatikainen, R.; Niemitz, M.; Weber, U.; Sundelin, J.; Hassinen, T.; Vepsäläinen, J. *J. Magn. Reson. A* **1996**, *120*, 1.

Table 1. Equilibrium Geometries, Harmonic Frequencies, and Cubic Anharmonic Force Fields for CX_2 (X = O, S, Se, Te)[a]

	CO_2			CS_2			CSe_2			CTe_2
	MP2[b]	CCSD(T)[c]	exptl	MP2[b]	CCSD(T)[d]	exptl[e]	MP2[b]	DFT[f]	exptl[g]	MP2[b]
r_e	1.1634	1.1626	1.1600[h]	1.5513	1.5596	1.5528	1.7053	1.689	1.692	1.9102
ω_1	1318.97	1352.0	1353.8[h]	675.41	670.05	673.42	371.84	381.78	374.48	261.56
ω_2	655.33	670.5	672.9[h]	369.74	398.63	398.40	299.65	307.06	302.89	238.77
ω_3	2311.68	2396.6	2396.5[h]	1552.60	1557.83	1558.71	1295.54	1305.01	1254.30	1149.10
f_{rr}	15.475	15.923	15.976[i]	8.133	7.777	7.881	6.228	6.448	6.088	5.027
$f_{rr'}$	0.920	1.159	1.232[i]	0.460	0.568	0.647	0.282	0.415	0.515	0.210
$f_{\theta\theta}$	0.792	0.762	0.778[i]	0.524	0.578	0.570	0.463	0.476	0.465	0.379
f_{rrr}	−105.185	−112.619	−116.8[i]	−42.954	−43.667	−44.095	−29.737	−36.053		−22.171
$f_{rrr'}$	−2.882	−2.712	−2.48[i]	−1.250	−1.097	−1.010	−0.810	−0.878		−0.409
$f_{r\theta\theta}$	−1.125	−1.121	−1.218[i]	−0.652	−0.738	−0.740	−0.477	−0.581		−0.413

[a] Geometries and force constants in units of Å, rad, and aJ. Frequencies in cm^{-1}. The isotopomers used for the frequencies are $^{13}C^{16}O_2$,$^{13}C^{32}S_2$, $^{13}C^{80}Se_2$, and $^{13}C^{130}Te_2$. [b] Present work. [c] Reference 55. [d] Reference 56. [e] Reference 57. Equilibrium geometry derived from the data of ref 57 in ref 56. [f] Reference 21. Harmonic frequencies calculated using the given force constants and geometries. [g] Reference 58. Harmonic frequencies calculated using the given force constants and geometries. [h] Reference 59. [i] Reference 60.

Table 2. Calculated ^{13}C Nuclear Magnetic Shielding Constants at the Equilibrium Geometry in CX_2 (X = O, S, Se, Te)[a]

				SO corrections						
molecule	theory	basis (C/X)	NR	FC(1)	FC(2)	SD(1+2)	FC-II(1)	SD-II(1)	Σ_{SO}	TOT
CO_2	DFT(PM)	HIII	58.62	0.55	−0.21		−0.39		−0.04	58.57
	DFT(CGO)	HIII		0.75	−0.28		−0.38		0.09	58.70[b]
	MCSCF	HIII	65.20	0.59		−0.18	−0.38	0.00	0.03	65.23
	MCSCF	HIVu3/HIV	64.73	0.58		−0.18	−0.40	0.00	0.00	64.73
	exptl									60.3[c]
CS_2	DFT(PM)	HIII	0.35	3.95	−0.78		−0.40		2.77	3.12
	DFT(CGO)	HIII		5.23	−1.02		−0.38		3.83	4.18[b]
	MCSCF	HIII	−11.97	5.37		−0.83	−0.37	0.00	4.18	−7.78
	MCSCF	HIVu3/HIV	−13.79	5.46		−0.86	−0.39	0.01	4.22	−9.57
	exptl									−5.9[c]
CSe_2	DFT(PM)	HIII	−43.99	26.61	−2.74		−0.39		23.48	−20.51
	DFT(CGO)	HIII		32.00	−3.17		−0.31		28.52	−15.47[b]
	MCSCF	HIII/HII	−55.71	39.21		−4.45	−0.29	0.00	34.47	−21.24
	MCSCF	HIVu3/HII	−56.09	39.22		−4.61	−0.30	0.01	34.31	−21.78
	exptl									−17.8,[d] −21.8[e]
CTe_2	DFT(PM)	HIII	−86.60	67.69	−3.94		2.83[f]		66.58	−20.02
	DFT(CGO)	HIII		82.97	−5.44		−0.26		77.27	−9.34[b]
	MCSCF	HIII/HII	−106.77	129.86		−12.70	−0.22	0.00	116.94	10.18
	MCSCF	HIVu3/HII	−107.73	129.66		−13.22	−0.24	0.00	116.21	8.48

[a] The nonrelativistic (NR) values and spin−orbit (SO) corrections are shown separately. Results in ppm. For NR results, either GIAO's (MCSCF) or IGLO PM (DFT) were used. For SO results, either common gauge origin (CGO) at the carbon atom (in all MCSCF calculations) or IGLO PM were used. For MCSCF, the one- and two-electron contributions are summed in the third-order terms. Calculations were performed using the optimized geometries given in Table 1. [b] Total shielding including the NR contribution calculated by the IGLO PM method. [c] Reference 61. Estimated equilibrium geometry gas-phase value. [d] Reference 21. Liquid-state experiment. [e] Reference 62. Solid state experiment. [f] The plateau of results for different values of λ_C only found for the summed SO correction FC(1) + FC−II(1).

4. Results and Discussion

4.1. Geometries and Force Fields. The optimized geometries are compared with literature values in Table 1, together with the full cubic anharmonic force field used in the work. The calculated structures are in good agreement with the best theoretical and experimental ones. There are some differences in the force constants between the different methods. For CO_2 and CS_2, the CCSD(T) calculations are closer to the experimental values. However, the present quasi-relativistic MP2/RECP results are not far away. We believe that the quality of the MP2 potential energy surface is sufficient for obtaining reliable rovibrational effects on the ^{13}C shielding tensor. The only previous force field calculation for the heavier members of the present series was the NR DFT work on CSe_2 in ref 21. The present MP2/RECP results are expected to be superior.

4.2. Spin−Orbit Coupling Effects at Equilibrium Geometry. The NR and SO contributions to the ^{13}C shielding constants at the equilibrium geometry are listed in Table 2. Table 3 shows the same for the shielding anisotropies. The DFT and MCSCF values for σ_C^{NR} differ and the deviation increases when going toward heavier X in the CX_2 series. This is most likely due to inaccuracies in both calculations. The DFT results depend on the choice of the approximate exchange-correlation functional, and compromises are made in the correlation treatment in the present MCSCF wave functions. For example, only the valence orbitals are correlated. On the basis of the results of ref 65 for related properties, correlating the outer-core/inner-valence orbitals can be expected to influence the MCSCF results, in particular for the SO corrections. On the other hand, it has in general been

(55) Martin, J. M. L.; Taylor, P. R.; Lee, T. J. *Chem. Phys. Lett.* **1993**, *205*, 535.
(56) Martin, J. M. L.; François, J.-P.; Gijbels, R. *J. Mol. Spectrosc.* **1995**, *169*, 445.
(57) Smith, D. F.; Overend, J. *J. Chem. Phys.* **1971**, *54*, 3632.
(58) Bürger, H.; Willner, H. *J. Mol. Spectrosc.* **1988,** *128*, 221.
(59) Teffo, J. L.; Sulakshina, O. N.; Perevalov, V. I. *J. Mol. Spectrosc.* **1992**, *156*, 48.
(60) Lacy, M. *Mol. Phys.* **1982**, *45*, 253.
(61) Jameson, A. K.; Jameson, C. J. *Chem. Phys. Lett.* **1987**, *134*, 461.
(62) Bernard, G. M.; Eichele, K.; Wu, G.; Kirby, C. W.; Wasylishen, R. E. W. *Can. J. Chem.* **2000**, *78*, 614.
(63) Spiess, H. W.; Schweizer, T.; Haeberlen, U.; Hausser, K. H. *J. Magn. Reson.* **1971**, *5*, 101.
(64) Jokisaari, J.; Lazzeretti, P.; Pyykkö, P. *Chem. Phys.* **1988,** *123*, 339.
(65) Lantto, P.; Vaara, J. *J Chem. Phys.* **2001**, *114*, 5482.

Table 3. Calculated ^{13}C Nuclear Magnetic Shielding Tensor Anisotropies in CX_2 (X = O, S, Se, Te)[a]

				SO corrections						
molecule	theory	basis C/X	NR	FC(1)	FC(2)	SD(1+2)	FC-II(1)	SD-II(1)	Σ_{SO}	TOT
CO_2	DFT(PM)	HIII	341.20	−0.82	0.31		−0.05		−0.56	340.64
	DFT(CGO)	HIII		−1.13	0.42		−0.05		−0.76	340.44[b]
	MCSCF	HIII	329.48	−0.88		0.22	−0.05	0.00	0.72	328.77
	MCSCF	HIVu3/HIV	329.78	−0.87		0.23	−0.05	0.00	0.70	329.07
CS_2	DFT(PM)	HIII	437.99	−5.92	1.17		−0.03		−4.78	433.21
	DFT(CGO)	HIII		−7.84	1.53		−0.05		−6.37	431.62[b]
	MCSCF	HIII	455.47	−8.06		0.91	−0.06	0.00	−7.21	448.26
	MCSCF	HIVu3/HIV	457.53	−8.19		0.94	−0.06	0.00	−7.31	450.22
	exptl									438(44)[c]
CSe_2	DFT(PM)	HIII	511.12	−39.91	4.11		0.02		−35.78	475.34
	DFT(CGO)	HIII		−47.99	4.76		−0.10		−43.34	467.75[b]
	MCSCF	HIII/HII	527.90	−58.81		5.15	−0.11	0.00	−53.77	474.12
	MCSCF	HIVu3/HII	527.97	−58.83		5.33	−0.11	0.00	−53.61	474.36
	exptl									506(30),[d] 506[e]
CTe_2	DFT(PM)	HIII	583.51	−101.53	5.90		−4.74[f]		−100.38	483.13
	DFT(CGO)	HIII		−124.45	8.14		−0.10		−116.41	467.10[b]
	MCSCF	HIII/HII	612.87	−194.80		15.41	−0.14	0.00	−179.53	433.33
	MCSCF	HIVu3/HII	613.91	−194.49		16.00	−0.14	0.00	−178.63	435.28

[a] See footnote *a* in Table 2. Anisotropy defined with respect to the direction of the molecular axis: $\Delta\sigma = \sigma_{\parallel} - \sigma_{\perp}$. [b] See footnote *b* in Table 2. [c] Reference 63. Spin−lattice relaxation experiment in the liquid state. [d] Reference 64. In liquid crystal solution. [e] See footnote *e* in Table 2. [f] See footnote *f* in Table 2.

found that DFT is better at producing relative chemical shifts than absolute shieldings (the latter are plagued by a systematic deshielding), particularly for atoms with many lone-pairs.[23,66,67] The magnitude of the DFT shieldings is smaller than that obtained using MCSCF for all molecules. For CO_2, the DFT result is deshielded relative to the MCSCF one by about 6.6 ppm. The situation is reversed for the heavier systems, with MCSCF giving negative, more deshielded NR results than DFT by 10 (CS_2) to 20 ppm (CTe_2). If the Loc.1 approximation of SOS-DFPT[23] with the modified energy denominators in σ^p is omitted, the DFT NR shieldings become more deshielded, reducing the gap to the MCSCF results to about the half (data not shown).

Based on the MCSCF results, the effect of improving the carbon basis from the HIII level is small. This holds also for the SO corrections. Hence, the HIII basis appears to be complete enough for the present purposes.

The different calculated NR results bracket the experimental σ_C for CO_2 and CS_2. In the case of CSe_2, however, the NR theory remains much too deshielded. There is no experiment for CTe_2. The SO contribution is positive and it increases as expected with the charge of the chalcogen nuclei, bringing the ^{13}C shielding closer to the experimental values for X = S and Se. In the MCSCF calculation of CTe_2, the SO correction is even larger than the NR shielding and therefore changes the sign of the total shielding. In particular, a good agreement with the experimental σ_C is obtained for CSe_2 after the SO corrections are taken into account.

The DFT method gives smaller SO effects than MCSCF. The difference increases toward heavier X. The treatment of the gauge origin problem affects the situation as the SO contribution increases from the IGLO PM calculation to the one where a CGO at carbon is employed, i.e., shifting the results toward the MCSCF values. The main cause of the remaining discrepancy of the DFT and MCSCF results is the smaller FC(1) contribution of DFT. This term is, similarly to the relatively small FC(2), quite sensitive to the correlation treatment. Without considering the third-order SD contributions that are calculated in the MCSCF but not in the DFT approach, the difference would be even larger. The SD terms diminish the total SO correction by more than 10%, and their relative importance increases toward lighter molecules. The second-order SO terms are quite similar in both the DFT and the MCSCF calculations. These contributions are very small and hence not numerically important in the present calculations. In the case of CTe_2, the FC-II(1) term seems to be smaller than for the lighter systems, indicating a small effect of this term on relative chemical shifts. Neglecting the Loc.1 approximation in the DFT calculations increases the total SO correction by up to more than 10% in CTe_2 (results not shown), improving again the agreement with the MCSCF data slightly.

The shielding anisotropy behaves in much the same way as the isotropic shielding. The anisotropy in CTe_2 is smaller than that in CSe_2 and even CS_2 due to the considerable increase of the SO contribution.

Summarizing, there are differences between the absolute shielding quantities calculated with the MCSCF and DFT methods due to the treatment of the gauge dependence, the fact that the SD contributions are neglected in the present DFT program, the difference in electron correlation treatment, and the SOS-DFPT corrections used in the DFT method. A detailed study of these effects for molecules containing elements beyond the first row would be of interest. For the present purposes, however, these discrepancies are expected to be systematic and constant for each molecule in the different conformations accessible to the rovibrational motion, as these sample the immediate vicinity of the equilibrium geometry. It is likely that the errors largely cancel when calculating the temperature evolution of the shieldings as well as the isotope effects, as these quantities involve differences of shielding constants at different geometries.

4.3. Rovibrational Effects on the ^{13}C Shielding Constants. The fitted parameters of the NR and SO carbon shielding surfaces and their contributions to the rovibrationally averaged property at 300 K are shown in Tables 4 and 5, respectively.

(66) Cheeseman, J. R.; Trucks, G. W.; Keith, T. A.; Frisch, M. J. *J. Chem. Phys.* **1996**, *104*, 5497.
(67) Rauhut, G.; Puyear, S.; Wolinski, K.; Pulay, P. *J. Phys. Chem.* **1996**, *100*, 6310.

Table 4. Calculated (DFT) Nonrelativistic ^{13}C Shielding Surfaces for CX_2 (X = O, S, Se, Te)[a]

	CO_2		CS_2			CSe_2		CTe_2	
	A	$\langle\sigma\rangle_A^{300\,K}$ [b]	A	$\langle\sigma\rangle_A^{300\,K}$ [b]	$\langle\sigma\rangle_A^{300\,K}$ [c]	A	$\langle\sigma\rangle_A^{300\,K}$ [b]	A	$\langle\sigma\rangle_A^{300\,K}$ [b]
σ_r^{NR}	−113.334	−1.146	−131.263	−1.322	−1.290	−135.214	−1.344	−158.430	−1.680
σ_{rr}^{NR}	−203.208	−0.242	−243.691	−0.348	−0.358	−594.144	−0.882	−300.655	−0.493
$\sigma_{rr'}^{NR}$	−162.311	0.063	−49.816	0.029	0.030	−155.328	0.107	−100.278	0.075
$\sigma_{\theta\theta}^{NR}$	−47.760	−0.428	−50.952	−0.503	−0.465	−38.430	−0.401	−73.988	−0.894
$\langle\sigma\rangle_{NR}^{0\,K} - \sigma_e$ [d]		−1.648		−1.797	−1.786		−1.974		−1.986
$\langle\sigma\rangle_{NR}^{300\,K} - \sigma_e$ [e]		−1.753		−2.145	−2.083		−2.521		−2.992

[a] The fitted parameters A and the corresponding contributions to the rovibrationally averaged property $\langle\sigma\rangle_A^{300\,K}$ at 300 K, are shown. Results in units of ppm, Å, and rad. [b] Contribution to averaged property at 300 K, equal to the product of the fitted parameter and the appropriate combination of linear or quadratic average displacement coordinates, eq 4. The isotopomers used are $^{13}C^{16}O_2$,$^{13}C^{32}S_2$, $^{13}C^{80}Se_2$, and $^{13}C^{130}Te_2$. The MP2/RECP force field from the present work was used. [c] Calculated using the CCSD(T) force field from ref 56. [d] Zero-point vibrational contribution. [e] Total rovibrational contributions at 300 K.

Table 5. Calculated (DFT) Spin−Orbit Correction Surfaces to ^{13}C Nuclear Shielding Constants in CX_2 (X = O, S, Se, Te)[a]

	CO_2		CS_2			CSe_2		CTe_2	
	A	$\langle\sigma\rangle_A^{300\,K}$	A	$\langle\sigma\rangle_A^{300\,K}$	$\langle\sigma\rangle_A^{300\,K}$	A	$\langle\sigma\rangle_A^{300\,K}$	A	$\langle\sigma\rangle_A^{300\,K}$
σ_r^{SO}	−0.186	−0.002	6.485	0.065	0.064	35.462	0.353	80.827	0.803
σ_{rr}^{SO}	41.994	0.050	28.686	0.041	0.042	334.277	0.496	919.229	0.560
$\sigma_{rr'}^{SO}$	−17.102	0.007	−26.564	0.016	0.016	52.690	−0.036	−135.240	0.117
$\sigma_{\theta\theta}^{SO}$	−0.445	−0.004	−2.544	−0.025	−0.023	24.138	0.252	167.531	1.010
$\langle\sigma\rangle_{SO}^{0\,K} - \sigma_e$		0.051		0.094	0.097		0.843		1.725
$\langle\sigma\rangle_{SO}^{300\,K} - \sigma_e$		0.051		0.097	0.099		1.065		2.490

[a] See footnotes in Table 4.

Also the total zero-point vibrational contributions are listed. The NR shielding derivatives are all negative, and there is a clearly increasing trend in magnitude of the σ_r parameter when going to the heavier molecules. The corresponding first-order term in eq 4 is responsible for over 50% of the total NR rovibrational corrections at 300 K. CSe_2 deviates from the trend of the other molecules where $\sigma_{\theta\theta}$ causes the second largest contribution. In CSe_2, σ_{rr} is particularly large while $\sigma_{\theta\theta}$ is quite small. Only the second-order cross-term contribution from $\sigma_{rr'}$ would be negligibly small in all these systems. Thermal effects, as indicated by the difference between the calculated values corresponding to 300 and 0 K, increase dramatically when going toward the heavier molecules, reaching about 50% of the 0 K value for CTe_2. The results from using the CCSD(T) force field of ref 54 for CS_2 are qualitatively similar to our MP2/RECP numbers, the major difference being in the slightly smaller thermal effects on σ_C^{NR}.

Rovibrational motion gives a *negative* contribution to the ^{13}C shielding constants at the NR level, and the contribution increases toward heavier X. On the contrary, most of the SO shielding derivatives are positive, hence the rovibrational contributions arising from the SO interaction *increase* the ^{13}C shielding constant.

The SO correction surface features clear increasing trends in the magnitude of σ_r and σ_{rr} when going toward heavier X. The first-order thermally averaged shielding contribution corresponding to σ_r is the dominant one for CS_2 (where the total SO effect is still small), and it is also important in CSe_2 and CTe_2. For CO_2 and CSe_2, σ_{rr} causes the largest contribution. In the case of CTe_2, the second-order $\sigma_{\theta\theta}$ term, corresponding to bending motion, is already larger than both of the previously mentioned contributions. The σ_{rr} contribution is almost of the same absolute magnitude in CSe_2 and CTe_2 and the difference in the total SO corrections for these two molecules is due to the σ_r and $\sigma_{\theta\theta}$ contributions. The angular contribution is negative for the two lightest molecules and positive for molecules containing heavy elements. As for the NR shielding, the $\sigma_{rr'}\langle\Delta r\Delta r'\rangle^T$ term is the least important for the SO corrections. The temperature effect on the SO corrections also increases with the nuclear charge of the chalcogen (both NR and SO effects are calculated from the same potential energy surface) and is about 45% for CTe_2 when comparing the total rovibrational correction at 300 K to the zero-point vibrational correction. For CO_2, there is practically no temperature effect on the SO correction.

If the Loc.1 approximation is not made, the magnitudes of both the NR- and SO-induced rovibrational corrections on the shielding constants increase by at most 15% in the heaviest molecules. For light main-group systems, the modified SOS-DFPT orbital energy denominators have empirically been found to improve the results. While this is not necessarily true for the heavier elements, we have chosen to use this approximation unless otherwise noted.

The temperature derivatives of the ^{13}C absolute shielding constants at 300 K are listed in Table 6. The present calculations correspond to isolated molecules in vacuo. The effect of the SO contribution on the temperature derivatives is negligible in CO_2 and CS_2. The calculated values for CO_2 are in absolute terms close to the experimental gas-phase value[68] appropriate to the isolated molecule. The present, very accurate experimental liquid-state temperature derivative in CS_2 is an order of magnitude larger than the calculated values. In CSe_2, the magnitude of the temperature derivative decreases by 40% due to the SO interaction, and the difference between the theoretical

(68) Jameson, C. J.; Jameson, A. K.; Parker, H.; Cohen, S. M.; Lee, C.-L. *J. Chem. Phys.* **1978,** *68*, 2861.

Table 6. Temperature Derivatives of the ^{13}C Nuclear Shielding Constants at 300 K[a]

method	CO_2	CS_2	CSe_2	CTe_2
DFT[b]	−0.8(−0.8)	−2.3(−2.3)	−1.9(−3.3)	−1.2(−5.5)
DFT[c]		−2.0(−2.0)		
exptl	−0.5369[d]	−14.2(2)[e]	−6.0[f]	

[a] All in ppb/K. Nonrelativistic value in parentheses. Same isotopomers as in Table 4. [b] Present calculations with the MP2/RECP force field. [c] Present calculations with the CCSD(T) force field.[56] [d] In gas phase. Reference 68. [e] Present experimental value in liquid state. Temperature derivative of the chemical shift (−13.9 ppb/K) relative to CH_4 is combined with the theoretical temperature dependence of σ_C (−0.26 ppb/K) in the (internal) reference molecule.[69] [f] In liquid C_6D_6 solution.[21]

Table 7. Experimental and Theoretical DFT Isotope Shifts for CO_2 at 300 K[a]

isotope shift	NR	SO	total	exptl[b]
$^1\Delta^{13}C(^{17}O,^{16}O)$	11.3	−0.3	11.0	
$^1\Delta^{13}C(^{18}O,^{16}O)$	21.4	−0.6	20.8	19(1)
$^1\Delta^{13}C(^{17}O,^{17}O)$	22.6	−0.6	22.0	
$^1\Delta^{13}C(^{18}O,^{17}O)$	32.8	−0.9	31.9	
$^1\Delta^{13}C(^{18}O,^{18}O)$	43.0	−1.2	41.8	39(3)

[a] In ppb. One-bond isotope shifts with respect to the $^{16}O{=}^{13}C{=}^{16}O$ isotopomer, i.e., $^1\Delta^{13}C(^{17}O,^{16}O) = \sigma_C(^{17}O,^{16}O) - \sigma_C(^{16}O,^{16}O)$ for the difference of the ^{13}C shielding constant in the isotopomers $^{17}O{=}^{13}C{=}^{16}O$ and $^{16}O{=}^{13}C{=}^{16}O$ (reference). [b] Gas-phase results from ref 70. The standard deviations are given (in parentheses) in units of the last digit.

and experimental[21] values increases as compared to the NR level. These facts point out that the experimental values from liquid samples contain significant contributions from solvent effects.[21] There are also uncertainties in the experimental values due to the indirect determination of the chemical shift relative to the reference molecule. The dependence of the absolute shielding on temperature and solvent effects in the reference molecule also influences the results.

An impressive SO effect is the calculated 80% decrease in CTe_2 which results in the second smallest temperature derivative in the present series, after CO_2. The ^{13}C shielding constant in CS_2 is the most sensitive to temperature and solvent effects in this series of molecules.

The effect of the choice of force field was tested for CS_2, as we computed the rovibrational averages also by using the accurate CCSD(T) cubic anharmonic force field by Martin et al.[56] The CCSD(T) force field produces total shielding corrections smaller in magnitude by about 1% at 0 K and 3% at 300 K, as compared to our force field. This is largely due to a change in the NR contribution. However, a larger effect of the choice of the force field is seen in the temperature derivative of the shielding at 300 K. The CCSD(T) force field diminishes the derivative by 13% when compared to the result obtained with the MP2/RECP force field.

The results for the temperature derivative of the absolute shielding display the difficulties in using this property as a means to compare theory and experiment. The situation is completely different for the isotope shifts discussed in the next section.

4.4. Isotope Shifts of the ^{13}C Shielding Constants. The secondary one-bond isotope shifts at 300 K are shown in Tables 7, 8, 9, and 10 for CO_2, CS_2, CSe_2, and CTe_2, respectively. The magnitude of both the NR and SO contributions to the isotope shifts of the ^{13}C shieldings increase linearly with the total mass of the molecule. This causes therefore a shift of the corresponding resonance toward lower frequency. The NR contributions are positive and the SO corrections decrease the magnitude of the total isotope shifts. The shift for symmetric isotopomers (i.e., with the same isotopes of the X nuclei) is about 5% larger than the shift of the isotopomer with the same mass but different isotopes of X.

Table 8. Experimental and Theoretical DFT Isotope Shifts for CS_2 at 300 K[a]

isotope shift	force field[b]	NR	SO	total	exptl
$^1\Delta^{13}C(^{33}S,^{32}S)$	MP2	3.9	−0.2	3.7	
	CCSD(T)	4.0	−0.2	3.8	
$^1\Delta^{13}C(^{34}S,^{32}S)$	MP2	7.5	−0.4	7.1	7.79(9)[c]
	CCSD(T)	7.7	−0.4	7.3	7.89(2)[d]
$^1\Delta^{13}C(^{33}S,^{33}S)$	MP2	7.7	−0.4	7.3	
	CCSD(T)	7.9	−0.4	7.5	
$^1\Delta^{13}C(^{34}S,^{33}S)$	MP2	11.4	−0.6	10.8	
	CCSD(T)	11.7	−0.6	11.1	
$^1\Delta^{13}C(^{36}S,^{32}S)$	MP2	14.2	−0.7	13.5	
	CCSD(T)	14.6	−0.7	13.9	
$^1\Delta^{13}C(^{34}S,^{34}S)$	MP2	15.0	−0.7	14.3	15.6(2)[c]
	CCSD(T)	15.4	−0.8	14.6	15.7(4)[d]
$^1\Delta^{13}C(^{36}S,^{33}S)$	MP2	18.1	−0.9	17.2	
	CCSD(T)	18.6	−0.9	17.7	
$^1\Delta^{13}C(^{36}S,^{34}S)$	MP2	21.8	−1.1	20.7	
	CCSD(T)	22.4	−1.2	21.2	
$^1\Delta^{13}C(^{36}S,^{36}S)$	MP2	28.5	−1.4	27.1	
	CCSD(T)	29.3	−1.5	27.8	

[a] In ppb. One-bond isotope shifts with respect to the $^{32}S{=}^{13}C{=}^{32}S$ isotopomer. See footnote *a* in Table 7. [b] MP2/RECP force field from the present work, the nonrelativistic CCSD(T) force field from ref 56. [c] Liquid-phase value in C_6D_6 solution.[71] [d] Present experimental value in liquid phase.

Table 9. Experimental and Theoretical Isotope Shifts for CSe_2 at 300 K[a]

isotope shift	spectral line[b]	NR	SO	total	exptl[c]	CAS[d]	BPW91[d]
$^1\Delta^{13}C(^{74}Se,^{74}Se)$		−6.6	2.7	−3.9		−6.0	−6.3
$^1\Delta^{13}C(^{74}Se,^{76}Se)$		−4.3	1.7	−2.6		−4.0	−4.2
$^1\Delta^{13}C(^{74}Se,^{78}Se)$	A	−2.2	0.9	−1.3	−1.2	−2.0	−2.1
$^1\Delta^{13}C(^{76}Se,^{76}Se)$	A	−2.1	0.9	−1.2	−1.2	−1.9	−2.0
$^1\Delta^{13}C(^{74}Se,^{80}Se)$	B	−0.2	0.1	−0.1	0.0	−0.2	−0.2
$^1\Delta^{13}C(^{74}Se,^{82}Se)$	C	1.7	−0.7	1.0	1.1	1.6	1.6
$^1\Delta^{13}C(^{76}Se,^{80}Se)$	C	2.0	−0.8	1.2	1.1	1.9	1.9
$^1\Delta^{13}C(^{78}Se,^{78}Se)$	C	2.1	−0.9	1.2	1.1	2.0	2.0
$^1\Delta^{13}C(^{76}Se,^{82}Se)$	D	3.9	−1.6	2.3	2.2	3.6	3.6
$^1\Delta^{13}C(^{78}Se,^{80}Se)$	D	4.1	−1.6	2.5	2.2	3.8	3.8
$^1\Delta^{13}C(^{78}Se,^{82}Se)$	E	6.0	−2.4	3.6	3.3	5.6	5.6
$^1\Delta^{13}C(^{80}Se,^{80}Se)$	E	6.1	−2.5	3.6	3.3	5.7	5.7
$^1\Delta^{13}C(^{80}Se,^{82}Se)$	F	8.1	−3.3	4.8	4.4	7.4	7.4
$^1\Delta^{13}C(^{82}Se,^{82}Se)$		10.0	−4.1	5.9		9.2	9.2

[a] In ppb. Isotope shifts with respect to the $^{76}Se{=}^{13}C{=}^{78}Se$ isotopomer. See the footnote *a* in Table 7. [b] See Figure 2a in ref 21. [c] Isotope shifts measured in liquid C_6D_6 solution.[21] [d] Nonrelativistic calculations reported in ref 21.

In comparison with experimental data, the NR calculation gives as expected reasonable isotope shifts for CO_2. While the small SO correction brings the total results closer to the experimental values, our approximations easily cause uncertainties of the same order of magnitude. The SO correction is 3% of the magnitude of the NR contribution. In the case of CS_2, the NR isotope shifts are already a bit smaller than the experimental ones. As the SO corrections reduce the total shift further, the agreement between theoretical and experimental shifts deteriorates slightly. Nevertheless, the theoretical calculations produce qualitatively correct isotope shifts. The effect of using the CCSD(T) force field[56] is an increase of about 3% in both NR and SO contributions as well as the total shift. Provided that the solvent effects are small (which is not necessarily the case), one can anticipate that the theoretical values would converge toward the experimental results if a state-of-the-art

Table 10. Theoretical DFT Isotope Shifts for CTe_2 at 300 K[a]

isotope shift	NR	SO	total
$^1\Delta^{13}C(^{123}Te,^{122}Te)$	0.3	−0.2	0.1
$^1\Delta^{13}C(^{124}Te,^{122}Te)$	0.7	−0.4	0.3
$^1\Delta^{13}C(^{123}Te,^{123}Te)$	0.7	−0.4	0.3
$^1\Delta^{13}C(^{125}Te,^{122}Te)$	1.1	−0.7	0.4
$^1\Delta^{13}C(^{124}Te,^{123}Te)$	1.1	−0.7	0.4
$^1\Delta^{13}C(^{126}Te,^{122}Te)$	1.4	−0.9	0.5
$^1\Delta^{13}C(^{124}Te,^{124}Te)$	1.4	−0.9	0.5
$^1\Delta^{13}C(^{125}Te,^{123}Te)$	1.4	−0.9	0.5
$^1\Delta^{13}C(^{126}Te,^{123}Te)$	1.8	−1.1	0.7
$^1\Delta^{13}C(^{125}Te,^{124}Te)$	1.8	−1.1	0.7
$^1\Delta^{13}C(^{128}Te,^{122}Te)$	2.1	−1.3	0.8
$^1\Delta^{13}C(^{125}Te,^{125}Te)$	2.2	−1.4	0.8
$^1\Delta^{13}C(^{126}Te,^{124}Te)$	2.2	−1.4	0.8
$^1\Delta^{13}C(^{128}Te,^{123}Te)$	2.5	−1.6	0.9
$^1\Delta^{13}C(^{126}Te,^{125}Te)$	2.5	−1.6	0.9
$^1\Delta^{13}C(^{130}Te,^{122}Te)$	2.8	−1.8	1.0
$^1\Delta^{13}C(^{128}Te,^{124}Te)$	2.8	−1.8	1.0
$^1\Delta^{13}C(^{126}Te,^{126}Te)$	2.8	−1.8	1.0
$^1\Delta^{13}C(^{130}Te,^{123}Te)$	3.1	−2.0	1.1
$^1\Delta^{13}C(^{128}Te,^{125}Te)$	3.2	−2.0	1.2
$^1\Delta^{13}C(^{130}Te,^{124}Te)$	3.5	−2.2	1.3
$^1\Delta^{13}C(^{128}Te,^{126}Te)$	3.5	−2.2	1.3
$^1\Delta^{13}C(^{130}Te,^{125}Te)$	3.8	−2.4	1.4
$^1\Delta^{13}C(^{130}Te,^{126}Te)$	4.2	−2.7	1.5
$^1\Delta^{13}C(^{128}Te,^{128}Te)$	4.2	−2.7	1.5
$^1\Delta^{13}C(^{130}Te,^{128}Te)$	4.9	−3.1	1.8
$^1\Delta^{13}C(^{130}Te,^{130}Te)$	5.5	−3.5	2.0

[a] In ppb. One-bond isotope shifts with respect to the $^{122}Te{=}^{13}C{=}^{122}Te$ isotopomer. See footnote *a* in Table 7.

ab initio shielding surface would be used with the CCSD(T) force field. The magnitude of the SO correction is 5% of the NR contribution and hence not negligible for CS_2. The present experimental values are slightly larger than the previous ones.[71] This can be due to the use of different solvents. However, both values are accurate enough for comparison with the calculated values.

There are both theoretical (NR) and experimental data by Lounila et al.[21] for CSe_2. The present NR shifts are slightly larger than the previously calculated complete active space (CAS) MCSCF and DFT results. The small difference may be due to the different gauge origin methods (presently IGLO and CGO and GIAO in ref 21), basis sets, correlation treatment (choice of the active orbital space and the exchange-correlation functional), and the calculated force fields. While the NR results overestimate the shift by a factor of 2 as already observed in ref 21, the present total isotope shifts converge practically to the experimental values when the SO correction is taken into account. The SO effect is 40% of the magnitude of the NR contribution. This is illustrated in Figure 1.

The dependence of the calculated total isotope shifts on the total mass of the isotopomer is slightly larger than observed experimentally, indicating that there may be room for improvements in the calculations. However, the present agreement with experiment offers convincing evidence for the importance of the SO contributions for secondary isotope effects on nuclear shieldings. For CTe_2, neither experimental nor theoretical data are available for comparison. Based on the results for the other molecules, we can expect that the present isotope shifts for ^{13}C

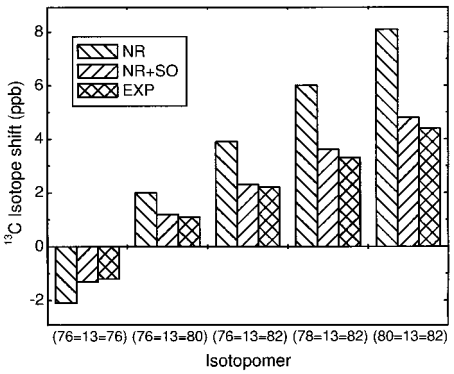

Figure 1. Comparison of the calculated (present work) and experimental[21] secondary one-bond isotope shifts on ^{13}C shielding for CSe_2 at 300 K. The reference is the $^{76}Se{=}^{13}C{=}^{78}Se$ isotopomer. The calculated shifts are presented both at the nonrelativistic (NR) level and with spin−orbit corrections (NR + SO).

Table 11. Temperature Derivatives of the Isotope Shifts of ^{13}C Nuclear Shielding Constant in CX_2 (X = O, S, Se, Te) at 300 K[a]

method	CO_2[b]	CS_2[c]	CSe_2[d]	CTe_2[e]
DFT[f]	−11.4(−11.4)	−10.2(−10.5)	−2.5(−4.3)	−0.7(−1.6)
DFT[g]		−10.4(−10.7)		
exptl		−10.9(3)[h]	−2[i]	

[a] Results in 10^{-3} ppb/K. SO-corrected results with the NR values in parentheses. [b] $\sigma_C(^{16}O,^{18}O) - \sigma_C(^{16}O,^{16}O)$. [c] $\sigma_C(^{32}S,^{34}S) - \sigma_C(^{32}S,^{32}S)$. [d] $\sigma_C(^{80}Se,^{80}Se) - \sigma_C(^{78}Se,^{80}Se)$ (E−D splitting in the spectrum of Figure 2a in ref 21). [e] $\sigma_C(^{130}Te,^{130}Te) - \sigma_C(^{128}Te,^{130}Te)$. [f] Present work with the MP2/RECP force field. [g] Present work with the CCSD(T) force field.[56] [h] Present value in liquid solution. [i] Previous value in liquid C_6D_6 solution.[21]

are reliable also for CTe_2. The magnitude of the SO correction is 65% of the NR contribution, and the SO effect therefore significantly reduces the magnitude of the isotope shifts in this molecule as well.

The SO effects on the temperature derivative of the main secondary isotope shifts on the ^{13}C shieldings at 300 K can be seen in Table 11. The SO interaction decreases the magnitude of the temperature derivative. In CS_2, the CCSD(T) force field increases the magnitude of the derivative by 2%. This is in the right direction as the experimental value is still somewhat larger. The experimental result is very sensitive to the quality of the spectra. Hence, the experimental value approached the calculated value as the measurements were improved. The SO effect in CS_2 is somewhat larger than in CO_2. The calculations predict a 3% SO contribution for the heavier molecule. The magnitude of the temperature derivative of the isotope shift decreases by 40% in CSe_2 due to the SO correction, in good agreement with the experimental value. The SO effect again explains the previously reported discrepancy by a factor of 2 between experimental and computed temperature derivatives.[21] Figures 2 and 3 illustrate the SO effect on the temperature dependence of representative ^{13}C isotope shifts in CS_2 and CSe_2, respectively. The SO correction does not change the slope of the isotope shift in CS_2 from the NR value. Its only effect is a downward displacement of the line describing the temperature dependence. Not only does the SO effect bring the isotope shifts close to the experimental values for CSe_2, but it also corrects the slope of the temperature dependence. The temperature derivative of the isotope shift of CTe_2 decreases by 55% due to the SO correction.

(69) Raynes, W. T.; Fowler, P. W.; Lazzeretti, P.; Zanasi, R.; Grayson, M. *Mol. Phys.* **1988**, *64*, 143.
(70) Wasylishen, R. E.; Friedrich, J. O.; Mooibroek, S.; Macdonald, J. B. *J. Chem. Phys.* **1985**, *83*, 548.
(71) Hiltunen, Y. *J. Magn. Reson.* **1991**, *92*, 170.

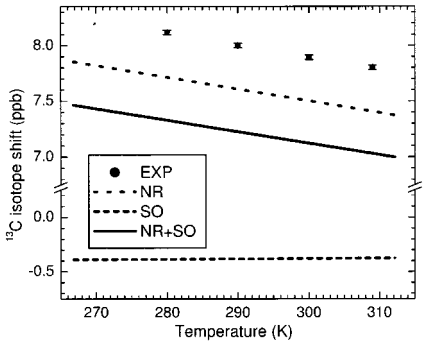

Figure 2. Calculated and experimental temperature dependence of the one-bond secondary isotope shift $\sigma_C(^{32}S,^{34}S) - \sigma_C(^{32}S,^{32}S)$ in CS_2. The experimental error limits are also shown.

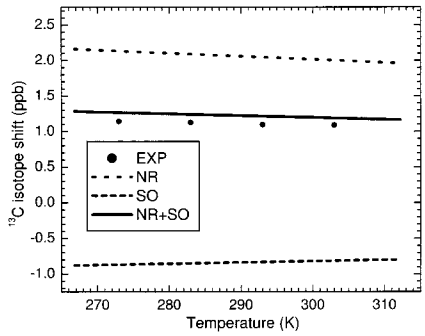

Figure 3. Calculated and experimental temperature dependence of the one-bond secondary isotope shift $\sigma_C(^{80}Se,^{80}Se) - \sigma_C(^{78}Se,^{80}Se)$ in CSe_2 (E−D splitting in the spectrum shown in Figure 2a of ref 21).

5. Conclusions

A theoretical first principles study of relativistic spin−orbit (SO) corrections to the secondary one-bond isotope effects on the ^{13}C nuclear shieldings in CX_2 (X = O, S, Se, Te) has been carried out. The harmonic and cubic anharmonic force constants have been used together with the calculated ^{13}C shielding hypersurfaces in the rovibrational averaging of the shielding. The shielding constants and their isotope shifts as well as their temperature dependence have been calculated and compared with experimental results.

The SO effects on the rovibrational corrections to ^{13}C nuclear shieldings—and thereby on the secondary isotope effects—can be significant, as has been anticipated in earlier work and demonstrated here. The SO interaction generally provides a contribution that diminishes the effects calculated at the nonrelativistic (NR) level. In CTe_2, the magnitude of the SO contribution is 65% of the magnitude of the NR contribution in the ^{13}C isotope shifts and 55% in the temperature dependence of the shifts. Hence, it is evident that one has to take SO coupling into account in calculations of the present properties for molecules containing heavy elements such as CSe_2 and CTe_2. The SO contribution brings the theoretical and experimental ^{13}C isotope shifts for CSe_2 into close agreement. The previously observed difference of a factor of 2 is shown to be fully due to the neglect of the SO effect, resulting in the overestimation of the isotope shifts and their temperature dependence.

In contrast, it is much more difficult to compare theory and experiment for the absolute shielding or its temperature dependence. The present underestimation of the temperature dependence of the absolute shielding in CSe_2 increases when taking the SO effect into account. This reflects problems in the experimental procedure, involving both the temperature dependence of the ^{13}C shielding in the reference molecule, and solvent effects on the investigated molecule as well as the reference molecule.

Through the experimentally convenient secondary isotope effects, the present work provides a novel demonstration of an important relativistic effect in chemistry.

Acknowledgment. J.V. thanks Prof. Pekka Pyykkö (Helsinki) and Dr. Juhani Lounila (Oulu) for discussions. P.L. is supported by the Alfred Kordelin Fund, Pohjois-Pohjanmaa Fund of the Finnish Cultural Foundation, and Vilho, Yrjö, and Kalle Väisälä Fund. J.V. is on leave from the NMR Research Group, Department of Physical Sciences, University of Oulu, Finland, and is supported by The Academy of Finland (grant 48578) and the Magnus Ehrnrooth Fund of the Finnish Society of Sciences and Letters. A.M.K. thanks the Finnish national graduate school of computational chemistry and molecular spectroscopy (LASKEMO) for funding. V.-V.T. and J.J. are also grateful to The Academy of Finland (grant 43979) for financial support. K.R. has been supported by the Norwegian Research Council by a postdoctoral fellowship (Grant No. 125851/410). The computational resources were partially provided by the Center for Scientific Computing, Espoo, Finland.

JA016537+